Landscape Ecol Eng (2016) 12:117–127
DOI 10.1007/s11355-013-0222-y

SPECIAL FEATURE - ORIGINAL PAPER

Landscape Design and Urban Biodiversity

Estimation of leaf area index and gap fraction in two broad-leaved forests by using small-footprint airborne LiDAR

Takeshi Sasaki · Junichi Imanishi · Keiko Ioki · Youngkeun Song · Yukihiro Morimoto

Received: 2 August 2012 / Revised: 26 February 2013 / Accepted: 9 April 2013 / Published online: 11 August 2013
© International Consortium of Landscape and Ecological Engineering and Springer Japan 2013

Abstract In this study, we evaluated methods for reliably estimating leaf area index (LAI) and gap fraction in two different types of broad-leaved forests by the use of airborne light detection and ranging (LiDAR) data. We evaluated 13 estimation variables related to laser height, laser penetration rate, and laser point attributes that were derived from LiDAR analyses. The relationships between LiDAR-derived estimates and field-based measurements taken from the forests were evaluated with simple linear regressions. The data from the two forests were analyzed separately and as an integrated dataset. Among the laser height variables, the coefficient of variation (CV) of all laser point heights had the highest level of accuracy for estimating both LAI and gap fraction. However, we recommend that more evaluations be conducted prior to the use of CV in forests with complex structures. The simplest laser penetration variable, which represents the ratio of the number of ground points to the total number of all points (P_{ALL}), also had a high level of accuracy for estimating LAI and gap fraction at the study sites regardless of whether the data were analyzed separately or as an integrated data set. Furthermore, P_{ALL} values showed near 1:1 relationships with the field-based gap fraction values. Hence, the use of P_{ALL} may be the most practical for estimating LAI and gap fraction in broad-leaved forests, even when the canopies are heavily closed.

Keywords Airborne laser scanner · Warm-temperate forest · Closed canopy · Laser penetration variable · Stable estimation method

T. Sasaki (✉) · J. Imanishi · Y. Song
Graduate School of Global Environment Studies, Kyoto University, Oiwake-cho, Kitashirakawa, Sakyo-ku, Kyoto 606-8502, Japan
e-mail: sasakita2@gmail.com

K. Ioki
Graduate School of Agricultural and Life Sciences, The University of Tokyo, 1-1-1 Yayoi, Bunkyo-ku, Tokyo 113-8657, Japan

Y. Morimoto
Faculty of Bio-Environmental Science, Kyoto Gakuen University, 1-1 Otani, Nanjo, Sogabe-cho, Kameoka, Kyoto 621-8555, Japan

Introduction

Forest leaf area index (LAI) and gap fraction are two important parameters that are used to describe forest structure. The LAI, which is defined as one half of the total leaf area per unit ground surface area (Jonckheere et al. 2004), correlates closely to the functions of photosynthesis and evapotranspiration, and it is used to model many processes related to carbon exchange and the regulation of climate by forests (Jonckheere et al. 2004; Hardin and Jensen 2007). Gap fraction, which represents the proportion of the forest canopy open to the sky and is the complement of canopy fractional cover, correlates closely to the penetration of solar radiation that affects the growth of forest biota such as seedlings (Nakamura et al. 2004). The accurate estimation of LAI and gap fraction is important for proper management to maximize and enhance the functions of forests. Unfortunately, costly and time-consuming field surveys are needed to estimate these parameters and these surveys can only be conducted over a limited spatial extent.

Remote sensing technology offers a cost-effective method for surveying wide areas of land. A number of research studies, using satellite and airborne passive optical remote sensing systems, have reported estimates of forest LAI and gap fraction (or fractional cover). Many researchers have used vegetation indices such as the normalized differential vegetation index (NDVI) (e.g., Nemani and Running 1989; Spanner et al. 1990; Chen and Cihlar 1996; Carlson and Ripley 1997; Cohen et al. 2003; Colombo et al. 2003). However, measurements collected by these passive optical remote sensing technologies have several disadvantages. For example, forestry data collected by passive remote sensing technology can be influenced by solar elevation angles and weather conditions, and such data often underestimate true LAI values because many of the vegetation indices become saturated at high levels of forest biomass and LAIs (Chen and Cihlar 1996).

Light detection and ranging (LiDAR) is an active remote sensing technology that directly obtains the distance between the sensor and a target surface by emitting laser pulses and determining the elapsed time between the emission and arrival of the signal (Lefsky et al. 2002). The use of LiDAR technology has increased greatly since the 1990s. One of the most important advantages of using LiDAR in forested areas is that the technology can acquire important data such as ground elevation inside the forest by penetrating the tree canopy. In other words, unlike passive optical remote sensing technologies, LiDAR instruments can acquire vertical, in addition to horizontal, information about the forest. Furthermore, measurements using LiDAR are less susceptible to shadows and weather conditions (Baltsavias 1999). Accordingly, the use of LiDAR technology could be very beneficial for deriving a cost-effective description of complex forest structures (Nelson et al. 1988; Lefsky et al. 2002).

Previous LiDAR-based studies have estimated forest structure parameters such as forest height (Popescu et al. 2002; Coops et al. 2007), biomass (Lim and Treitz 2004; Næsset and Gobakken 2008), and timber volume (Packalén and Maltamo 2006; Donoghue et al. 2007). Several studies have also estimated forest LAI, gap fraction, and fractional cover using various indices derived from LiDAR data such as laser height metrics and laser penetration rates of the canopy (Riaño et al. 2004; Morsdorf et al. 2006; Sasaki et al. 2008; Richardson et al. 2009).

A few studies have attempted to establish regional scale LiDAR models that would be applicable for use over two or more forested areas. Jensen et al. (2008) estimated LAIs in two conifer forests using LiDAR and SPOT5 data, and found that LiDAR-only models can account for a significant amount of the variation in field-based LAI measurements for individual study areas and also when generalized over larger regions. Hopkinson and Chasmer (2009) tested models to estimate fractional cover across multiple forests using LiDAR-based metrics related to the laser penetration of canopies. While these studies are valuable, more studies of this nature are needed to validate the use of this promising technology for regional forestry applications. Especially, more studies are needed from different types of forests for the establishment of robust LiDAR estimation methods.

The development of LiDAR estimation methods for broad-leaved forests, which are common in Japan, has been limited. In this study, we targeted two broad-leaved forests in Japan and aimed to establish robust methods for estimating LAI and gap fraction values that would be applicable for use in different types of broad-leaved forests. This was accomplished by comparing 13 LiDAR estimation variables related to laser height, laser penetration rate, and laser point attributes to field-based measurements of LAI and gap fraction.

Methods

Study sites

The study area was comprised of two distinct forests in the Kansai region of Japan (Fig. 1). Both forests were located in the warm-temperate zone where the climax vegetation consisted of evergreen broad-leaved trees.

The Expo '70 Commemorative Park (135°31′32′E, 34°47′48′N) is located in Suita City, Osaka Prefecture. After the World Exposition in 1970, the site was covered with imported local soils from the neighboring hills. The park was re-vegetated over a period from 1972 to 1976 (Morimoto et al. 2006) with evergreen broad-leaved trees and some deciduous broad-leaved trees. Presently, more than 30 years after the reclamation, the planted trees have reached heights of up to 20 m. The main tree species include *Quercus glauca*, *Cinnamomum camphora*, and *Castanopsis cuspidata* in the evergreen stands, and *Quercus serrata*, *Quercus acutissima*, and *Prunus jamasakura* in the deciduous stands. The ground elevation of the park varies moderately between 40 and 61 m above sea level. The area of the evergreen broad-leaved forest covers approximately 0.291 km^2, and the area of deciduous broad-leaved forest covers approximately 0.045 km^2.

Constructed in 1655, the Shugakuin Imperial Villa (135°48′E, 35°03′N) is located in the city of Kyoto, Kyoto Prefecture. The mountainous forest surrounding the villa was incorporated into the design of the villa's gardens as "borrowed scenery," and it is managed for aesthetic purposes. This forest covers an area of approximately 0.544 km^2, and it has a complex topography that varies between 100 and 343 m above sea level. For our research, we targeted the broad-leaved stands in the forest that consisted primarily of deciduous tree species including *Quercus serrata*, *Quercus variabilis*, and *Ilex pedunculos*,

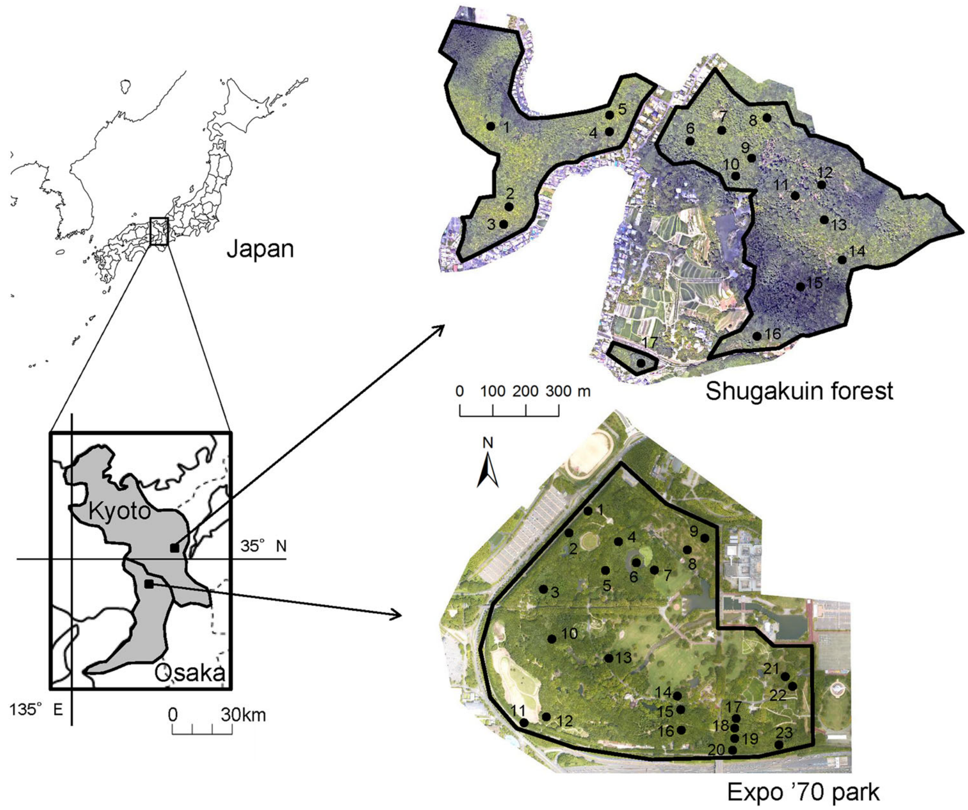

Fig. 1 Locations of the study sites and plots where field measurements were taken

and a few evergreen species including *Quercus glauca* and *Cleyera japonica*.

Hereafter, we refer to the Expo '70 Commemorative Park as the "Expo '70 park," and the mountainous forest surrounding the Shugakuin Imperial Villa as the "Shugakuin forest."

Field data collection

We established 23 study plots in the Expo '70 park (E1–E23) and 17 plots in the Shugakuin forest (S1–S17) (Fig. 1; Table 1). The plot sizes ranged from 100 m^2 (10 m × 10 m) to 400 m^2 (20 m × 20 m) depending on the tree density and the topography of the stands. Hemispherical photographs were taken at five or more points in each plot using a digital Coolpix 995 camera (Nikon Co., Tokyo, Japan) equipped with a FC-E8 fish-eye lens (Nikon Co.) leveled on a tripod 1.3 m above the ground. We avoided large trees that were nearby when taking field measurements to prevent their irregular influence. We took at least three photographs with different exposures at each measurement point, and used the most representative photograph (i.e., the one that had a good contrast between the sky and foliage) in our analyses. The measurements were conducted during overcast weather conditions between the months of July and September in 2008. The locations of all of the plots were determined using a GPS system (GPS Pathfinder ProXH, Trimble Navigation Ltd., California, USA) and a pocket compass (Tracon LS-25, Ushikata Co., Yokohama, Japan). Because of the steeper terrain in the Shugakuin forest, the slope for each plot was measured at the center of the plot to take into consideration the influence of topography.

The gap fraction was calculated from photographs using CanopOn 2 software (Takenaka 2009). This software divides a hemispherical photograph into 11 annulus rings that are split at 8.6°, 16.0°, 24.3°, 32.4°, 40.9°, 49.9°, 57.8°, 65.0°, 73.2°, 81.7°, and 90.0°. The software calculates 11 gap fraction values according to integrated annuli from 0–8.6° to 0–90.0°. We calculated the gap fraction within the range that was not influenced by topography in each plot.

The effective LAI values were calculated for each integral annulus with a program that calculates LAI values using an assumption of a spherical leaf angle distribution based on that of Norman and Campbell (1989). The effective LAI is the value of the LAI when the canopy is assumed to be randomly distributed (Jonckheere et al. 2004). For broadleaf canopies, the effective LAI is often adopted as a substitute for the true LAI (e.g., Muraoka and Koizumi 2005; Riaño et al. 2004). Hereafter, we report the calculated effective LAI simply as the LAI.

Table 1 Field inventory and results of ground-based measurement in each plot with the annulus range of 0–32.4°

Plot	Dominant species	LAI		Gap fraction	
		Mean	SD	Mean	SD
Expo '70 park					
E1	*Quercus phillyraeoides* A. Gray	4.81	0.35	0.076	0.012
E2	*Quercus phillyraeoides*	5.70	0.34	0.048	0.007
E3	*Cinnamomum camphora* (L.) Presl, *Quercus glauca* Thunb. ex Murray	4.92	1.30	0.095	0.037
E4	*Castanopsis cuspidata* (Thunb. ex Murray) Schottky, *Quercus glauca*	5.74	0.64	0.055	0.014
E5	*Ulmus parvifolia* Jacquin, *Celtis sinensis* Pers. var. japonica (Planch.) Nakai	5.34	1.24	0.073	0.025
E6	*Machilus thunbergii* Sieb. Et Zucc., *Quercus myrsinifolia* Blume	5.86	0.97	0.049	0.013
E7	*Quercus glauca*, *Machilus thunbergii*	6.94	0.71	0.029	0.010
E8	*Prunus* × *yedoensis* Matsumura	1.58	0.44	0.446	0.074
E9	*Castanopsis sieboldii* (Makino) Hatusima ex Yamazaki et Mashiba, *Celtis sinensis* var. japonica	6.65	0.41	0.035	0.009
E10	*Quercus glauca*, *Quercus phillyraeoides*	5.04	0.72	0.070	0.026
E11	*Quercus phillyraeoides*	4.80	0.30	0.082	0.010
E12	*Quercus acutissima* Carruthers	3.98	0.24	0.140	0.009
E13	*Quercus glauca*, *Cinnamomum camphora*	5.91	0.86	0.050	0.016
E14	*Quercus serrata* Thunb. ex Murray	3.12	0.46	0.191	0.028
E15	*Quercus acutissima*, *Prunus jamasakura* Sieb. ex Koidz	3.39	0.61	0.166	0.045
E16	*Quercus glauca*, *Cinnamomum camphora*	5.14	0.82	0.071	0.011
E17	*Quercus glauca*, *Ligustrum japonicum* Thunb.	5.26	0.58	0.063	0.014
E18	*Castanopsis cuspidata*, *Machilus thunbergii*	5.61	0.53	0.054	0.008
E19	*Machilus thunbergii*, *Quercus glauca*	5.12	0.43	0.069	0.011
E20	*Quercus phillyraeoides*	5.03	0.52	0.077	0.010
E21	*Quercus serrata*, *Prunus jamasakura*	3.71	1.22	0.162	0.069
E22	*Quercus serrata*, *Prunus jamasakura*	2.82	0.47	0.215	0.045
E23	*Cinnamomum camphora*	4.44	0.34	0.099	0.013
Shugakuin forest					
S1	*Ilex pedunculosa* Miq.	4.36	0.49	0.102	0.020
S2	*Ilex pedunculosa*, *Lyonia ovalifolia* (Wall.) Drude var. elliptica (Sieb. Et Zucc.) Hand.—Mazz	3.97	0.72	0.138	0.043
S3	*Quercus variabilis* Blume, *Quercus glauca*	5.84	0.90	0.057	0.019
S4	*Quercus serrata*, *Quercus acutissima*	5.30	0.26	0.068	0.009
S5	*Ilex pedunculosa*, *Quercus serrata*	5.59	0.27	0.052	0.007
S6	*Symplocos prunifolia* Sieb. et Zucc., *Ilex pedunculosa*	4.78	0.51	0.092	0.013
S7	*Cleyera japonica* Thunb., *Ilex pedunculosa*	4.13	0.60	0.110	0.038
S8	*Ilex pedunculosa*, *Acanthopanax sciadophylloides* Franch. et Savat.	4.65	0.36	0.099	0.015
S9	*Ilex pedunculosa*, *Photinia glabra* (Thunb.) Maxim.	4.42	0.98	0.115	0.036
S10	*Cleyera japonica*	3.78	0.54	0.139	0.036
S11	*Quercus serrata*	7.46	1.43	0.029	0.011
S12	*Acanthopanax sciadophylloides*	2.95	1.03	0.230	0.137
S13	*Quercus variabilis*, *Quercus glauca*	5.87	0.81	0.060	0.015
S14	*Quercus acutissima*, *Evodiopanax innovans* (Sieb. et Zucc.) Nakai	4.59	0.96	0.097	0.042
S15	*Quercus acutissima*, *Carpinus laxiflora* (Sieb. et Zucc.) Bl.	5.62	1.37	0.063	0.035
S16	*Quercus glauca*	5.04	1.31	0.083	0.031
S17	*Prunus jamasakura*	4.18	1.93	0.163	0.124

Scientific names after Satake et al. (1989)

LiDAR data collection and processing

The airborne LiDAR data were collected over the study areas using a RIEGL LMS-Q560 sensor (Riegl Laser Measurement Systems GmbH, Horn, Austria) mounted on a helicopter platform on July 23, 2008 (Shugakuin forest) and August 22, 2008 (Expo '70 park). This system projects near-infrared laser beams (1,550 nm) and records the full waveform of the reflection. The pulse frequency was 150 kHz and the scanning angle was ±30°. The flying height was 300 m above ground level and the beam divergence was 0.5 mrad, yielding a ground footprint of approximately 0.15 m in diameter. The flight speed was around 92.6 km h^{-1}. A back-and-forth flight pattern was conducted to survey the entire area.

The full-waveform data from the entire area were converted into discrete points using the RiANALYZE software of RIEGL (RIEGL Laser Measurement Systems GmbH, 2009) by the Nakanihon Air Service Co., Ltd., Japan. This software detects local amplitude maxima above a certain threshold value by applying Gaussian pulse estimation. All of the created points have *x*, *y*, and *z* coordinate values and any of the following attributes: "first," "intermediate," "last," or "only" returns. The attributes "first," "intermediate," and "last" returns refer to the order in which the projected laser hits the canopy components while passing through the canopy. If all of the energy of a projected laser is returned at the same time, it is recorded as an "only" return. All created points have intensity values representing the reflected pulse energy amplitude.

Terrascan software (TerraSolid Ltd., Helsinki, Finland) was used for processing the point cloud data. For all points, we derived the height above the ground using a 0.5 m mesh digital elevation model (DEM) created by building a triangulated surface model. The points 1.3 m above the ground were classified as "vegetation" points, and the residual points as "ground" points. The threshold of 1.3 m is the height at which the lens was placed when we took the hemispherical photographs. Note that the classes the "ground" and "vegetation" are independent of the point echo types (i.e., first, intermediate, last, and only returns) for the raw data.

The predictor variables related to laser point height, laser penetration rate, and laser point attributes were calculated for individual plots (Table 2). The laser height variables included the mean (MEAN), maximum (MAX), standard deviation (SD), and coefficient of variation (CV) of all return heights, and the mean ($\mathrm{MEAN_{VEG}}$), standard deviation ($\mathrm{SD_{VEG}}$), and coefficient of variation ($\mathrm{CV_{VEG}}$) of vegetation return heights. For the laser penetration rate, we calculated the following five variables:

$$P_{\mathrm{ALL}} = \frac{N_{\mathrm{Ground}}}{N_{\mathrm{All}}}$$

$$P_{\mathrm{FO}} = \frac{N_{\mathrm{GroundFirst}} + N_{\mathrm{GroundOnly}}}{N_{\mathrm{First}} + N_{\mathrm{Only}}}$$

$$P_{\mathrm{LO}} = \frac{N_{\mathrm{GroundLast}} + N_{\mathrm{GroundOnly}}}{N_{\mathrm{Last}} + N_{\mathrm{Only}}}$$

$$\mathrm{PI} = \frac{I_{\mathrm{Ground}}}{I_{\mathrm{All}}}$$

$$\mathrm{PI_{BL}} = \frac{\left(\frac{I_{\mathrm{GroundOnly}}}{I_{\mathrm{All}}}\right) + \sqrt{\frac{I_{\mathrm{GroundLast}}}{I_{\mathrm{All}}}}}{\left(\frac{I_{\mathrm{First}} + I_{\mathrm{Only}}}{I_{\mathrm{All}}}\right) + \sqrt{\frac{I_{\mathrm{Intermediate}} + I_{\mathrm{Last}}}{I_{\mathrm{All}}}}}$$

where N_{All}, N_{Ground}, N_{First}, N_{Last}, and N_{Only} represent the number of all points, ground points, "first" returns, "last" returns, and "only" returns for individual plots, respectively. We also counted the number of "first", "last", and "only" returns within the ground points ($N_{\mathrm{GroundFirst}}$, $N_{\mathrm{GroundLast}}$, and $N_{\mathrm{GroundOnly}}$). The parameters I_{All}, I_{Ground}, I_{First}, $I_{\mathrm{Intermediate}}$, I_{Last}, and I_{Only} represent the sum of intensity values of all points, ground points, "first" returns, "intermediate" returns, "last" returns, and "only" returns, respectively. The parameters $I_{\mathrm{GroundLast}}$ and $I_{\mathrm{GroundOnly}}$ represent the sum of intensity values of "last" and "only" returns within the ground points respectively. The $\mathrm{PI_{BL}}$ is the complement of the $\mathrm{FC_{Lidar(BL)}}$, which is the Beer's Law modified fractional cover equation proposed by Hopkinson and Chasmer (2009). This equation takes into consideration the fact that intermediate and last returns are residual energies after previous returns in the travel paths of the emitted laser pulses, and are attenuated in both incoming and outgoing transmission processes.

For the laser point attributes, we calculated the following variable:

$$A_{\mathrm{VO}} = \frac{N_{\mathrm{VegetationOnly}}}{N_{\mathrm{VegetationFirst}} + N_{\mathrm{VegetationOnly}}}$$

where $N_{\mathrm{VegetationFirst}}$ and $N_{\mathrm{VegetationOnly}}$ represent the numbers of "first" returns and "only" returns within the vegetation points, respectively.

Statistical analyses

A simple linear regression analysis was used to evaluate the strength of the relationship between the LiDAR data collected from Expo '70 park and Shugakuin forest and field-based measurements of LAI and gap fraction. The data from the two forests were analyzed separately and as an integrated dataset. Leave-one-out-cross-validation (LOOCV) was performed, and the predicted residual sum of squares (PRESS) was calculated. The efficiencies of predictor variables were examined by the use of coefficients of determination (R^2) and root mean square errors (RMSEs) that accounted for the results of the LOOCV.

Table 2 Results of regression analysis of LiDAR variables with LAI and gap fraction

Variable	Expo '70		Shugakuin		Integrated	
	PRESS R^2	RMSEv	PRESS R^2	RMSEv	PRESS R^2	RMSEv
LAI						
Height variables						
MEAN	−0.015	1.235	0.511	0.704	0.315	0.942
MAX	−0.143	1.311	0.239	0.879	0.008	1.134
SD	0.310	1.018	−0.156	1.083	−0.036	1.159
CV	0.775	0.582	0.449	0.747	0.706	0.617
$MEAN_{VEG}$	−0.158	1.319	0.463	0.738	0.215	1.009
SD_{VEG}	0.269	1.048	−0.103	1.058	−0.083	1.185
CV_{VEG}	0.681	0.693	0.201	0.900	0.515	0.793
Penetration variables						
P_{ALL}	0.696	0.676	0.503	0.710	0.582	0.736
P_{FO}	−0.063	1.264	0.045	0.984	−0.108	1.198
P_{LO}	0.683	0.690	0.297	0.845	0.548	0.766
PI	0.210	1.090	0.307	0.839	0.150	1.049
PI_{BL}	0.679	0.695	0.379	0.794	0.572	0.745
Attribute variable						
A_{VO}	0.761	0.600	−0.131	1.071	0.428	0.861
Gap fraction						
Height variables						
MEAN	−0.037	0.090	0.399	0.036	0.186	0.066
MAX	−0.126	0.093	0.120	0.044	−0.029	0.075
SD	0.156	0.081	−0.164	0.051	−0.024	0.074
CV	0.783	0.041	0.596	0.030	0.771	0.035
$MEAN_{VEG}$	−0.145	0.094	0.349	0.038	0.110	0.069
SD_{VEG}	0.130	0.082	−0.146	0.050	−0.066	0.076
CV_{VEG}	0.724	0.046	0.252	0.041	0.540	0.050
Penetration variables						
P_{ALL}	0.884	0.030	0.733	0.024	0.841	0.029
P_{FO}	0.723	0.046	0.018	0.047	0.584	0.047
P_{LO}	0.903	0.027	0.594	0.030	0.853	0.028
PI	0.944	0.021	0.583	0.030	0.831	0.030
PI_{BL}	0.903	0.027	0.546	0.032	0.839	0.030
Attribute variable						
A_{VO}	0.586	0.057	−0.071	0.049	0.447	0.055

Specifically, these were PRESS R^2 and $RMSE_V$. All statistical analyses were performed using R version 2.13.1 software (R Development Core Team 2011).

Results

Determination of the best hemispherical photograph annulus

Figure 2 shows examples of cross-sectional LiDAR returns for each study site. All plots in the Expo '70 park were on relatively flat topography, whereas many plots in the Shugakuin forest were on a steep terrain. Because the steepest plot in the Shugakuin forest exhibited a slope of 41.2°, we excluded annuli over 40.9° from the hemispherical photographs to avoid the influence of topography when calculating gap fraction and LAI. In addition to the influence of topography, large annuli can cause sampling errors by including adjoining stands, while small annuli can cause the dispersion of values in each plot because they are limited to observing only the narrow area directly overhead of the camera. In consideration of these issues, we chose to use data from the annulus range of 0–32.4° in our study. Table 1 shows the mean values and standard deviations of field measurements of LAI and gap fraction for each plot.

Fig. 2 Example cross-sectional LiDAR (light detection and ranging) returns for each study site; E4 (Expo '70 park) and S9 (Shugakuin forest)

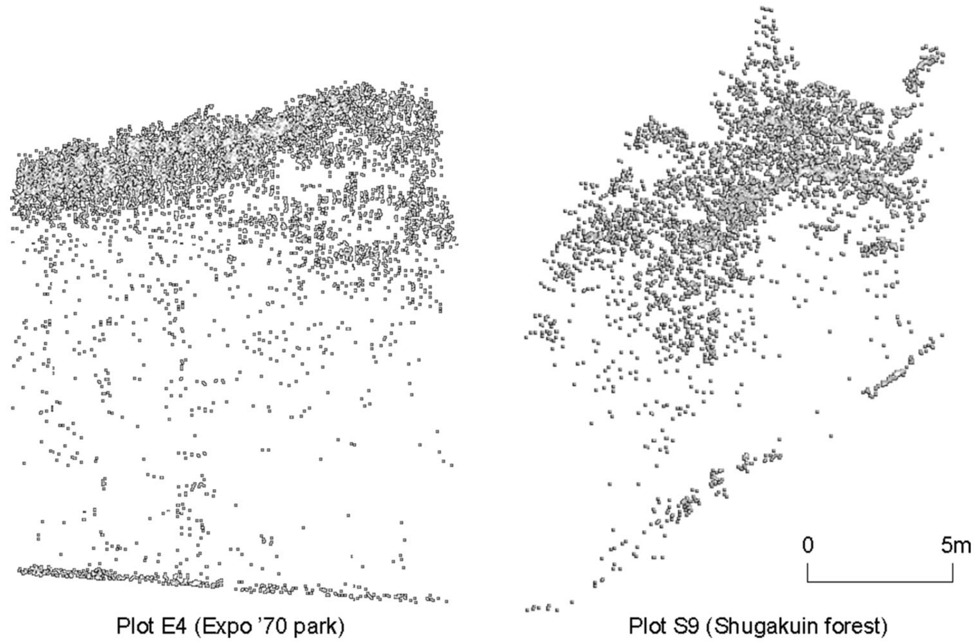

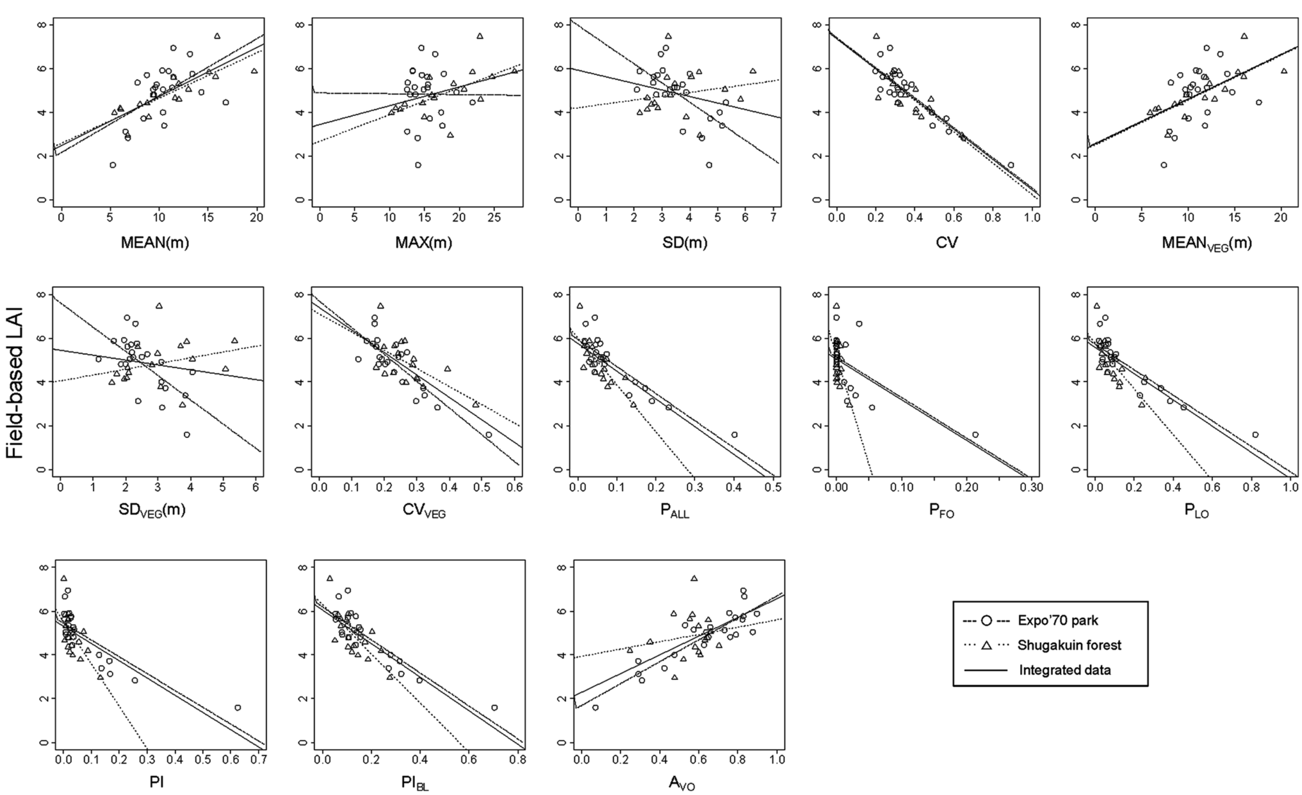

Fig. 3 Scatter diagrams and regression lines showing the relationships between LiDAR-based variables and field-based LAI (leaf area index) values

LAI estimation

Table 2 shows the results of regression analyses between the LiDAR-based variables and the field-based measurements LAI and gap fraction for the Expo '70 park, the Shugakuin forest, and the integrated dataset. The scatter diagrams and regression lines are illustrated in Fig. 3 (LAI) and Fig. 4 (gap fraction).

Among the laser height variables, the CV had the best LAI estimation accuracies for the Expo '70 park data

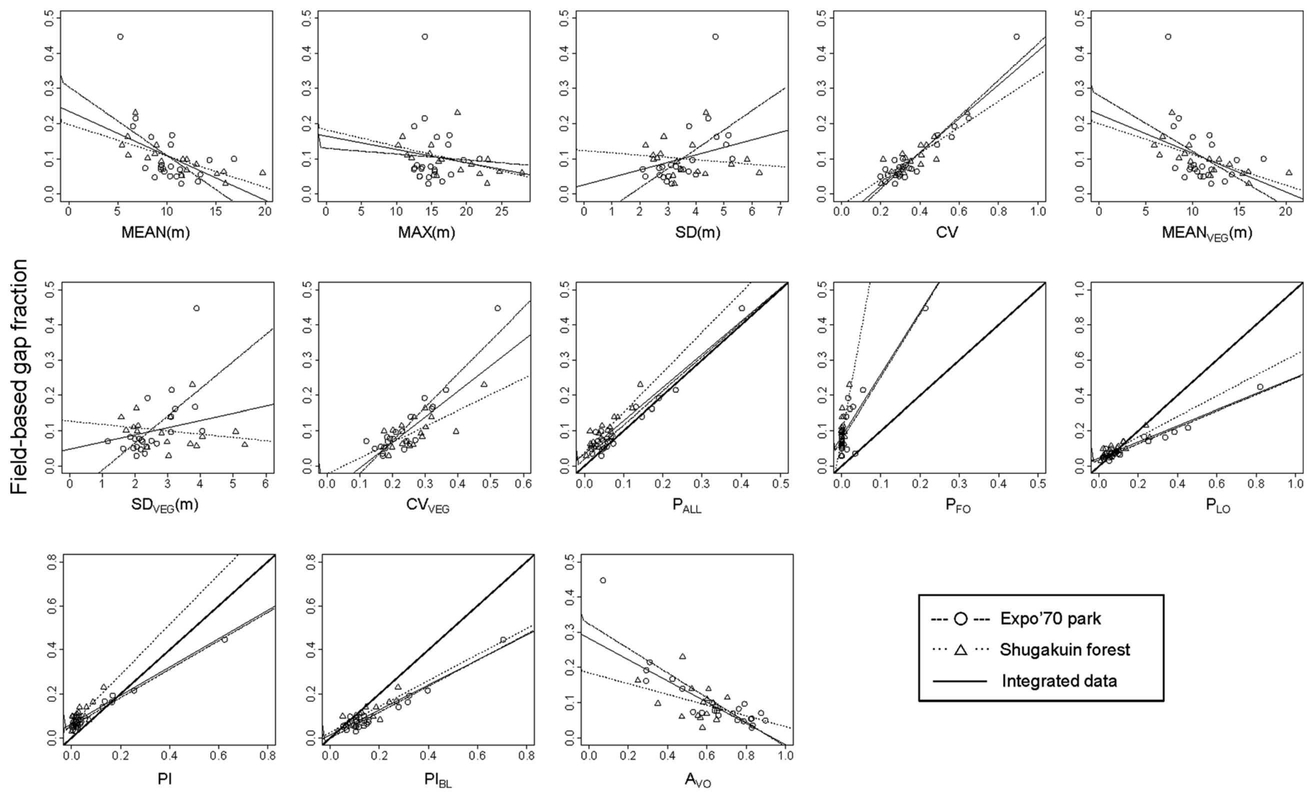

Fig. 4 Scatter diagrams and regression lines showing the relationships between LiDAR-based variables and field-based gap fraction values. The *bold lines* in several of the diagrams (e.g., for laser penetration variables P_{ALL}, P_{FO}, P_{LO}, PI, PI_{BL}) indicate a 1:1 relationship

(PRESS $R^2 = 0.775$, RMSEv = 0.582) and the integrated data (PRESS $R^2 = 0.706$, RMSEv = 0.617), and the third highest accuracy for the Shugakuin forest data (PRESS $R^2 = 0.449$, RMSEv = 0.747). The MEAN had the highest accuracy for the Shugakuin forest data (PRESS $R^2 = 0.511$, RMSEv = 0.704), but it was not effective in the Expo '70 park (PRESS $R^2 < 0$). The $MEAN_{VEG}$ and CV_{VEG}, respectively, had lower accuracies than the MEAN and CV in all datasets. The MAX, SD, and SD_{VEG} had low estimation accuracies in all datasets.

In regards to the laser penetration variables, P_{ALL} had the highest PRESS R^2 values (Expo '70 = 0696; Shugakuin = 0.503; Integrated = 0.582) and the lowest RMSEv values (Expo '70 = 0676; Shugakuin = 0.710; Integrated = 0.736) in all datasets. The estimation accuracies of P_{FO} and PI were low in all datasets. As for P_{LO} and PI_{BL}, the PRESS R^2 values were higher than 0.6 for the Expo '70 park data and higher than 0.5 in the integrated dataset.

The laser attribute variable, termed A_{VO}, showed a high estimation accuracy for the Expo '70 park data (PRESS $R^2 = 0.761$, RMSEv = 0.600), but a low accuracy for estimating LAI in the Shugakuin forest.

Gap fraction estimation

Among the laser height variables, the CV showed the highest PRESS R^2 values (Expo '70 = 0.783; Shugakuin = 0.596; Integrated = 0.771) and lowest RMSEv values (Expo '70 = 0.041; Shugakuin = 0.030; Integrated = 0.035) in all the datasets. The CV_{VEG} had the second highest accuracies for the Expo '70 park data and the integrated data, but low accuracy in Shugakuin forest. The other height values, MEAN, MAX, SD, $MEAN_{VEG}$, and SD_{VEG}, showed low estimation accuracies.

For the laser penetration variables, the estimation accuracies were higher in the Expo '70 park than in the Shugakuin forest. The estimation accuracies for gap fraction were higher than those for LAI for almost all variables analyzed except for P_{FO}, which had low estimation accuracies for both LAI and gap fraction in the Shugakuin forest (see Table 2). The variable, P_{ALL}, had stable and high PRESS R^2 values (Expo '70 = 0.884; Shugakuin = 0.733; Integrated = 0.841) and low RMSEv values (Expo '70 = 0.030; Shugakuin = 0.024; Integrated = 0.029). We used bold lines to highlight 1:1 relationships in the diagrams depicting laser penetration variables in Fig. 4. The results of regression analyses between P_{ALL} and gap fraction showed a near 1:1 relationship for the Expo '70 park data and the integrated data, although the P_{ALL} underestimated the gap fraction for the Shugakuin forest data. The P_{FO} exhibited small values and became zero for five plots in the Expo '70 park and six plots in the Shugakuin forest, resulting in a marked underestimation of the gap fraction. As for the other variables, P_{LO}, PI, and PI_{BL}, the PRESS R^2 values were higher than 0.9 for the Expo '70 park data and higher than 0.5 for the Shugakuin forest data, although the regression lines deviated from 1:1 relationships.

For A_{VO}, a relatively high estimation accuracy was shown in the Expo '70 park (PRESS $R^2 = 0.586$, RMSEv $= 0.057$), but a low A_{VO} accuracy was seen in the Shugakuin forest (Table 2). This pattern was similar to what was observed for LAI estimates.

Discussion

Laser height variables

Among the laser height variables, the CV had the highest levels of accuracy for estimating both LAI and gap fraction, with the exception of LAI estimation in the Shugakuin forest. The CV represents the relative dispersion of the vertical laser point height distribution, which has been shown to be a good predictor for discriminating among stands of different canopy densities (Donoghue et al. 2007; Bater et al. 2009). In dense forests, many laser points concentrate in the upper canopy and few laser pulses reach the ground, resulting in small CV values. In contrast, if the canopy has few leaves, most laser pulses penetrate the canopy and reach the ground resulting in the dispersion of point height and larger CV values. The CV_{VEG} showed lower estimation accuracies than the CV. This was likely because the ground returns emphasized the vertical dispersion of height in low-density plots, resulting in larger variances of CV than CV_{VEG}. (Figs. 3, 4).

The estimation accuracies for CV values in the Expo '70 park were higher than in the Shugakuin forest. The trees of the Expo '70 park were planted during a short period in the 1970s, and many plots are now dominated by evergreen broad-leaved trees of similar height. These plots also have heavily closed canopies and poor stratification structures (Morimoto et al. 2006). This type of homogeneity in the forest structure may have led to distinctly small CV values. On the other hand, the use of CV was less reliable for estimating the LAI of the Shugakuin forest (i.e., the PRESS R^2 value was <0.5) (Table 2). This may have been a result of the complex vertical stratifications of some plots in the Shugakuin forest, where increases in the LAI did not always lead to an increase of canopy surface density.

Therefore, these results suggest that the CV is not a variable that is directly related to leaf abundance, and it can be affected by forest stratification structures such as those in the sub-canopy and shrub layers. In consideration of these findings, we recommend that more evaluations be conducted prior to the use of CV for estimating LAI and gap fraction, especially in forests with complex structures.

Laser penetration variables

The laser penetration variables showed higher accuracies in estimating gap fraction than in estimating LAI. According to Beer's law, the gap fraction decreases exponentially as the LAI increases, and small variations in low gap fraction values correspond to large variations in the LAI. In this study, most of the plots that we analyzed had closed canopies and gap fractions that were lower than 0.2 (Table 1). These characteristics seemed to amplify errors in the LAI values. In addition, the estimation accuracies of the laser penetration variables were higher in the Expo '70 park than in the Shugakuin forest (Table 2). This was likely because the Expo '70 park had a gentle topography and a more homogeneous forest structure within each plot that led to a reduction in estimation errors, whereas the Shugakuin forest had steep slopes and a more heterogeneous forest structure.

In past studies, the complement of the P_{FO} has been used for estimations of LAI and canopy cover (Miura and Jones 2010; Korhonen et al. 2011). However, this was not possible in the present study because P_{FO} values were very small in many plots. The practical use of the P_{FO} for estimating forest structure in the broad-leaved forests examined in this study was limited due to their closed canopies and high LAI values (>5) in many plots (Table 1). Because the laser footprint (0.15 m) used in this study was larger than the small gaps in closed forest canopies, most of the "first" returns and "only" returns likely hit the tops of the canopies, and missed many of the small gaps (Solberg et al. 2009). Interestingly, the P_{LO} had higher estimation accuracies than the P_{FO}. This could possibly be because the P_{LO} simply targets the returns that penetrated the canopy, and is less sensitive to dense canopies compared to the P_{FO}. Although, the P_{LO} tended to overestimate high gap fraction values (Fig. 4). This may be because the P_{LO} ignores the first hit on the canopy surface, which can cause overestimation when the canopy gap is sufficient enough in size that laser beams can penetrate the canopy.

Consistent with past studies on individual forests (Sasaki et al. 2008; Richardson et al. 2009), estimations accuracies by P_{ALL} were stable and high for both LAI and gap fraction values in all datasets. Furthermore, correlations between P_{ALL} and gap fraction had near 1:1 relationships. The use of all returns provided a sufficient sample density, and seemed to offset any tendencies for underestimation when using "first" returns and overestimation when using "last" returns. These results imply that the simplest penetration variable, P_{ALL}, would be useful for deriving stable estimates of LAI and gap fraction in broad-leaved forests.

With regard to the variables based on intensity data, the PI showed low accuracies for estimating the LAI, but this was improved by using the PI_{BL}. These improvements likely resulted because any errors were mitigated by taking into consideration the energy losses associated with each laser point attribute (Hopkinson and Chasmer 2009). For gap fraction estimation, the PI had PRESS R^2 values >0.9 for the Expo '70 park and >0.5 for the Shugakuin forest, but the PI values were lower than 0.1 for many plots (Figs. 3, 4). This was mitigated to some extent by the use of the PI_{BL} (Figs. 3, 4). In contrast to the case described by Hopkinson and Chasmer (2009), the relationships we observed between PI_{BL} and field-based gap fraction values deviated from 1:1 relationships. A possible reason for this is that the intensity represents the reflection value of infrared laser beams (1550 nm), and this value can differ depending on the objects that are hit (i.e., such as vegetation and ground), and the types of trees and plant species that are present in the study area.

Laser attribute variable

The variable, $A_{VO,}$ showed high estimation accuracies in the Expo '70 forest, but low accuracies in the Shugakuin forest for both LAI and gap fraction. Because many stands in the Expo '70 park are composed of similar-aged trees, the plots dominated by evergreen broad-leaved tree species had less canopy surface roughness (Fig. 2). This resulted in many "only" returns hitting the canopy surface at the same time within a given footprint area. In contrast, the Shugakuin forest is a secondary forest that has been managed for a long time, and it contains many plots with higher amounts of canopy surface roughness regardless of leaf abundance levels. This aspect of the forest structure likely resulted in less "only" returns. In consideration of these observations, A_{VO} appears to be a less stable estimation parameter when compared to the other laser penetration variables, and it seems useful only for forests that have relatively homogeneous structures and uniform tree heights.

Conclusions

In this study, we evaluated methods for reliably estimating LAI and gap fraction in two different types of broad-leaved forests by the use of airborne LiDAR data. Among the predictor variables, the CV had high estimation accuracies, but it was less effective when targeting forests that had complex vertical structures. The simplest laser penetration variable, P_{ALL}, also had a high level of accuracy for estimating both LAI and gap fraction at the two study sites regardless of whether the data were analyzed separately or as an integrated data set. The P_{ALL} values showed near 1:1 relationships with the field-based gap fraction values. Additionally, the use of P_{ALL} has been shown to be valuable in past studies of individual forests. These findings suggest that P_{ALL} estimates may be the most stable indicators to use in various types of forest. Hence, we conclude that P_{ALL} may be the most practical LiDAR-based variable to use for estimating LAI and gap fraction in broad-leaved forests.

Acknowledgments We wish to acknowledge the staff of the Commemorative Organization for the Japan World Exposition '70 and Japanese Imperial Household Agency for their support in field observation.

References

Baltsavias EP (1999) A comparison between photogrammetry and laser scanning. ISPRS J Photogramm 54:83–94

Bater CW, Coops NC, Gergel SE, LeMay V, Collins D (2009) Estimation of standing dead tree class distributions in northwest coastal forests using lidar remote sensing. Can J Forest Res 39:1080–1091

Carlson TN, Ripley DA (1997) On the relation between NDVI, fractional vegetation cover, and leaf area index. Remote Sens Environ 62:241–251

Chen JM, Cihlar J (1996) Retrieving leaf area index of boreal conifer forests using Landsat TM images. Remote Sens Environ 55:153–162

Cohen WB, Maiersperger TK, Gower ST, Turner DP (2003) An improved strategy for regression of biophysical variables and Landsat ETM + data. Remote Sens Environ 84:561–571

Colombo R, Bellingeri D, Fasolini D, Marino CM (2003) Retrieval of leaf area index in different vegetation types using high resolution satellite data. Remote Sens Environ 86:120–131

Coops NC, Hilker T, Wulder MA, St-Onge B, Newnham G, Siggins A, Trofymow JA (2007) Estimating canopy structure of Douglas-fir forest stands from discrete-return LiDAR. Trees Struct Funct 21:295–310

Donoghue DNM, Watt PJ, Cox NJ, Wilson J (2007) Remote sensing of species mixtures in conifer plantations using LiDAR height and intensity data. Remote Sens Environ 110:509–522

Hardin PJ, Jensen R (2007) The effect of urban leaf area on summertime urban surface kinetic temperatures: a Terre Haute case study. Urban For Urban Gree 6:63–72

Hopkinson C, Chasmer L (2009) Testing LiDAR models of fractional cover across multiple forest ecozones. Remote Sens Environ 113:275–288

Jensen JLR, Humes KS, Vierling LA, Hudak AT (2008) Discrete return lidar-based prediction of leaf area index in two conifer forests. Remote Sens Environ 112:3947–3957

Jonckheere I, Fleck S, Nackaerts K, Muys B, Coppin P, Weiss M, Baret F (2004) Review of methods for in situ leaf area index

determination: part I. Theories, sensors and hemispherical photography. Agric Forest Meteorol 121:19–35
Korhonen L, Korpela I, Heiskanen J, Maltamo M (2011) Airborne discrete-return LIDAR data in the estimation of vertical canopy cover, angular canopy closure and leaf area index. Remote Sens Environ 115:1065–1080
Lefsky MA, Cohen WB, Parker GG, Harding DJ (2002) Lidar remote sensing for ecosystem studies. Bioscience 52:19–30
Lim KS, Treitz PM (2004) Estimation of above ground forest biomass from airborne discrete return laser scanner data using canopy-based quantile estimators. Scand J Forest Res 19:558–570
Miura N, Jones SD (2010) Characterizing forest ecological structure using pulse types and heights of airborne laser scanning. Remote Sens Environ 114:1069–1076
Morimoto Y, Njoroge JB, Nakamura A, Sasaki T, Chihara Y (2006) Role of the EXPO '70 forest project in forest restoration in urban areas. Lands Ecol Eng 2:119–127
Morsdorf F, Kotz B, Meier E, Itten KI, Allgower B (2006) Estimation of LAI and fractional cover from small footprint airborne laser scanning data based on gap fraction. Remote Sens Environ 104:50–61
Muraoka H, Koizumi H (2005) Photosynthetic and structural characteristics of canopy and shrub trees in a cool-temperate deciduous broadleaved forest. Agric Forest Methodol 134:39–59
Næsset E, Gobakken T (2008) Estimation of above- and below-ground biomass across regions of the boreal forest zone using airborne laser. Remote Sens Environ 112:3079–3090
Nakamura A, Morimoto Y, Mizutani Y (2004) Adaptive management approach to increasing the diversity of a 30-year-old planted forest in an urban area of Japan. Landsc Urban Plan 70:291–300
Nelson R, Krabill W, Tonelli J (1988) Estimating forest biomass and volume using airborne laser data. Remote Sens Environ 24:247–267
Nemani RR, Running SW (1989) Testing a theoretical climate-soil-leaf area hydrologic equilibrium of forests using satellite data and ecosystem simulation. Agric Forest Methodol 44:245–260
Norman JM, Campbell GS (1989) Canopy structure. In: Pearcy RW, Ehleringer JR, Mooney HA, Rundel PW (eds) Plant physiological ecology: field methods and instrumentation. Chapman and Hall, London, pp 301–325
Packalén P, Maltamo M (2006) Predicting the plot volume by tree species using airborne laser scanning and aerial photographs. Forest Sci 52:611–622
Popescu SC, Wynne RH, Nelson RF (2002) Estimating plot-level tree heights with lidar: local filtering with a canopy-height based variable window size. Comput Electron Agr 37:71–95
R Development Core Team (2011) R: a language and environment for statistical computing. R Foundation for Statistical Computing, Vienna. ISBN: 3-900051-07-0. http://www.R-project.org
Riaño D, Valladares F, Condes S, Chuvieco E (2004) Estimation of leaf area index and covered ground from airborne laser scanner (Lidar) in two contrasting forests. Agric Forest Methodol 124:269–275
Richardson JJ, Moskal LM, Kim SH (2009) Modeling approaches to estimate effective leaf area index from aerial discrete-return LIDAR. Agric Forest Methodol 149:1152–1160
Sasaki T, Imanishi J, Ioki K, Morimoto Y, Kitada K (2008) Estimation of leaf area index and canopy openness in broad-leaved forest using airborne laser scanner in comparison with high-resolution near-infrared digital photography. Landsc Ecol Eng 4:47–55
Satake Y, Hara H, Watari S, Tominari T (1989) Wild flowers of Japan: woody plants I and II, 1st edn. Heibonsha Ltd. Publishers, Tokyo
Solberg S, Brunner A, Hanssen KH, Lange H, Næsset E, Rautiainen M, Stenberg P (2009) Mapping LAI in a Norway spruce forest using airborne laser scanning. Remote Sens Environ 113:2317–2327
Spanner MA, Pierce LL, Running SW, Peterson DL (1990) The seasonality of AVHRR data of temperate coniferous forests: relationship with leaf area index. Remote Sens Environ 33:97–112
Takenaka A (2009) CanopOn2. http://takenaka-akio.cool.ne.jp/etc/canopon2/. Accessed 25 July 2012